

**Nuclear polarization effects in big bang nucleosynthesis**Victor T. Voronchev<sup>1,\*</sup> and Yasuyuki Nakao<sup>2,†</sup><sup>1</sup>*Skobeltsyn Institute of Nuclear Physics, Lomonosov Moscow State University, Moscow 119991, Russia*<sup>2</sup>*Green Asia Education Center, Kyushu University 6-1 Kasuga-koen, Kasuga, Fukuoka 816-8580, Japan*

(Received 14 April 2015; published 15 October 2015)

A standard nuclear reaction network for big bang nucleosynthesis (BBN) simulations operates with spin-averaged nuclear inputs—unpolarized reaction cross sections. At the same time, the major part of reactions controlling the abundances of light elements is spin dependent, i.e., their cross sections depend on the mutual orientation of reacting particle spins. Primordial magnetic fields in the BBN epoch may to a certain degree polarize particles and thereby affect some reactions between them, introducing uncertainties in standard BBN predictions. To clarify the points, we have examined the effects of induced polarization on key BBN reactions— $p(n, \gamma)d$ ,  $d(d, p)t$ ,  $d(d, n)^3\text{He}$ ,  $t(d, n)\alpha$ ,  $^3\text{He}(n, p)t$ ,  $^3\text{He}(d, p)\alpha$ ,  $^7\text{Li}(p, \alpha)\alpha$ ,  $^7\text{Be}(n, p)^7\text{Li}$ —and the abundances of elements with  $A \leq 7$ . It has been obtained that the magnetic field with the strength  $B_0 \leq 10^{12}$  G (at the temperature of  $10^9$  K) has almost no effect on the reaction cross sections, and the spin polarization mechanism plays a minor role in the element production, changing the abundances at most by 0.01%. However, if the magnetic field  $B_0$  reaches  $10^{15}$  G its effect on the key reactions appears and becomes appreciable at  $B_0 \gtrsim 10^{16}$  G. In particular, it has been found that such a field can increase the  $p(n, \gamma)d$  cross section (relevant to the starting point of BBN) by a factor of 2 and at the same time almost block the  $^3\text{He}(n, p)t$  reaction responsible for the interconversion of  $A = 3$  nuclei in the early Universe. This suggests that the spin polarization effects may become important in nonstandard scenarios of BBN considering the existence of local magnetic bubbles inside which the field can reach  $\sim 10^{15}$  G.

DOI: 10.1103/PhysRevD.92.083008

PACS numbers: 24.70.+s, 26.35.+c, 95.30.-k

**I. INTRODUCTION**

In 2003, Spergel *et al.* [1] reported the first experimental data on the baryon density of the Universe  $\Omega_b$  derived from WMAP observations. These findings radically changed the status of the standard model of big bang nucleosynthesis (standard BBN or SBBN), making it a parameter-free theory providing a remarkable tool for the early Universe probe. The sole free parameter originally incorporated in SBBN [2,3]—the number density of baryons  $n_b$  normalized to the number density of background black body photons  $n_\gamma$ , that is,  $\eta = n_b/n_\gamma$ —has been no longer considered free as it is uniquely related to the baryon density by  $\Omega_b h^2 = 3.65 \times 10^7 \eta$ . It is not surprising therefore that rigorous simulations of SBBN with the baryon-to-photon ratio  $\eta_{\text{WMAP}}$  obtained at different stages of the WMAP mission [1,4–6] have been carried out. They demonstrated that the standard model gives good agreement between predicted and observed abundances of D and  $^4\text{He}$ , but essentially overestimates the amount of primordial  $^7\text{Li}$  by a factor of 3–4 [7]. Furthermore, a recent update of abundances [12] with cosmological parameters obtained from Planck observations [13] did not modify the overall picture of primordial nucleosynthesis, slightly decreasing the lithium abundance by a few percent [14].

Various nuclear-physical issues have been explored to date to improve accuracy of SBBN predictions. Not being able to consider all papers in the field, we note some recent studies, classifying them into three general categories:

- (1) *Reaction data.*—Main nuclear inputs, such as reaction cross sections  $\sigma$  and/or reaction rate parameters  $\langle \sigma v \rangle$ , were carefully revised for processes most important to the production of light elements up to beryllium (see, e.g., [16–20]). A significant extension of the nuclear database to reactions involving higher- $Z$  nuclei up to oxygen was recently reported in [21]. At the same time, considerable attention was paid to resonant destruction of  $A = 7$  isotopes in the context of the cosmological  $^7\text{Li}$  problem. Theoretical papers here were particularly focused on searching for low-energy resonances in  $x + ^7\text{Be}$  nuclear systems ( $x = d, t, ^3\text{He}, \alpha$ ) and on their possible impact on the  $^7\text{Li}$  abundance [22–25]. However, the “missing” resonances were not clearly observed in the latest experiments [26,27]. One more issue widely discussed in the literature is variations of fundamental constants determining nuclear interaction at the time of BBN. For details, we refer the reader to papers [28,29] and references therein.
- (2) *Reaction network.*—A standard BBN network [30] commonly employed in benchmark calculations operates with almost 90 reactions for 26 nuclides.

\*voronchev@srd.sinp.msu.ru

†nakao@nucl.kyushu-u.ac.jp

For the past few years however the network has been significantly improved by adding a large number of reactions previously neglected. In particular, more than 100 reactions were added by Iocco *et al.* [31] while Coc *et al.* [21] extended the network to nearly 400 processes for 59 nuclides. These authors carried out comprehensive calculations of the element production up to the carbon-nitrogen-oxygen group. Given a high number density  $n_e$  of electron-positron pairs in the BBN epoch ( $n_e \sim 10^{27} \text{ cm}^{-3}$  at temperature of  $10^9 \text{ K}$ ), electrodisintegration processes for loosely bound nuclei  $d$ ,  ${}^7\text{Li}$ ,  ${}^7\text{Be}$  were also incorporated in the BBN network. However, the  $d(e, e'n)p$  disintegration rate was estimated [32] to be much smaller than the rate of competing  $d(\gamma, n)p$  photonuclear reaction. Similar results were recently obtained for electro- and photodisintegrations of  ${}^7\text{Li}$  and  ${}^7\text{Be}$  [33].

- (3) *Reaction peculiarities in plasma.*—Several kinds of reaction peculiarities can manifest in the primordial plasma due to interaction of reacting nuclei with ambient particles. One of them is electron screening of nuclear reactions at deep sub-barrier energies. However, it was recently demonstrated [34] that this effect does not produce a noticeable impact on light element abundances. Another kind of peculiarities is reactions with excited nuclei, i.e., processes proceeding through thermally populated low-lying states of reacting particles. In particular, thermal excitation of  ${}^7\text{Be}$  in the plasma and its possible influence on  ${}^7\text{Be}$  depletion were discussed in [20]. Besides these factors, a number of recent studies were focused on non-Maxwellian distortions of particle distribution functions and their effects on BBN. We can note a paper [35], where the Tsallis nonextensive statistics was employed for nucleosynthesis simulations. Non-Maxwellian nuclear effects triggered by energetic particles produced in  $d + t$ ,  $d + {}^3\text{He}$ , and  $d + d$  fusion reactions in the primordial plasma were examined in [20,36–38]. It was concluded [38] that these particles can significantly increase the rates of some reactions, but the respective corrections to light element abundances prove to be less than 1%.

Apart from the above issues, some specific effects triggered by primordial magnetic fields (PMFs) in the BBN epoch attract noticeable attention. The physics of PMF and its influence on BBN have been widely discussed in the literature [39–51]. The PMF action has been rigorously analyzed in matters of weak reaction rates, electron and positron thermodynamics, the Universe expansion rate, etc. In the meantime, there remains a nuclear-physical question which has not been studied in detail yet. It is spin polarization of plasma particles by the PMF (induced nuclear polarization) and its effect on some

TABLE I. Nuclear reactions most important to the production of light elements in SBBN (Nos. 1–11). Processes sensitive to the spin orientation of reacting particles are marked by symbol  $\checkmark$ .

| No. | Reaction                    |              | No. | Reaction                                     |              |
|-----|-----------------------------|--------------|-----|--|--------------|
| 1   | $p(n, \gamma)d$             | $\checkmark$ | 7   | ${}^3\text{He}(d, p)\alpha$                  | $\checkmark$ |
| 2   | $d(p, \gamma){}^3\text{He}$ | $\checkmark$ | 8   | $t(\alpha, \gamma){}^7\text{Li}$             |              |
| 3   | $d(d, p)t$                  | $\checkmark$ | 9   | ${}^3\text{He}(\alpha, \gamma){}^7\text{Be}$ |              |
| 4   | $d(d, n){}^3\text{He}$      | $\checkmark$ | 10  | ${}^7\text{Li}(p, \alpha)\alpha$             | $\checkmark$ |
| 5   | $t(d, n)\alpha$             | $\checkmark$ | 11  | ${}^7\text{Be}(n, p){}^7\text{Li}$           | $\checkmark$ |
| 6   | ${}^3\text{He}(n, p)t$      | $\checkmark$ | 12  | ${}^7\text{Be}(n, \alpha)\alpha$             | $\checkmark$ |

reaction cross sections [52] and the primordial element production. It is well known that the spin of particle with magnetic moment  $\mu$  has a tendency to “line up” along (for  $\mu > 0$ ) or opposite (for  $\mu < 0$ ) the direction of magnetic field  $B$ . Therefore, the sufficiently strong PMF may change the rates of two-body reactions whose cross sections depend on mutual orientation of reacting particle spins. In relation with this one should emphasize that most of the key reactions controlling the abundances of light elements in SBBN just belong to the above type of processes (see Table I).

In the present paper we analyze spin polarization effects in BBN. The paper is organized as follows. In Sec. II, a treatment of nuclear reactions with spin-polarized particles is discussed. In Sec. III, we calculate the degree of particle polarization in the primordial plasma and clarify whether spin-polarized reactions can affect light element abundances. The magnetic field influence on the cross sections of some individual reactions is also discussed. The main conclusions of our study are summarized in Sec. IV.

## II. TREATMENT OF REACTIONS WITH SPIN-POLARIZED PARTICLES

Let us introduce a quantity to be used to describe the degree of nucleus polarization by the PMF. The alignment of nucleus spin in an external magnetic field  $B$  is commonly characterized by the nuclear polarization factor  $P_{\text{nuc}}$  [53]:

$$P_{\text{nuc}} = \frac{1}{I} \sum_m m \xi(m) \equiv \frac{1}{I} \langle m \rangle, \quad (1)$$

where  $I$  is the spin,  $m (= I, I-1, \dots, -I)$  is its projection onto a quantization axis coinciding with the field direction  $\mathbf{n}_B$ , and  $\xi(m)$  is the probability that the nucleus is in the  $m$  state. It is given by

$$\xi(m) = \frac{\exp[-\epsilon(m)/T]}{\sum_{m'} \exp[-\epsilon(m')/T]}, \quad \sum_m \xi(m) = 1, \quad (2)$$

where  $\epsilon(m)$  is the energy of magnetic sublevel,

$$\epsilon(m) = -m\mu B/I, \quad (3)$$

and  $T$  is temperature expressed in units of energy. In Eq. (3),  $\mu$  is the nucleus magnetic moment and  $B$  is the magnetic field strength. To determine the degree to which the PMF can affect reaction cross sections, one needs to properly incorporate  $\xi(m)$  in a description of nuclear processes sensitive to mutual orientation of reacting particle spins. In the present study we focus on several spin-dependent reactions marked by symbol  $\checkmark$  in Table I. All of them (except the reaction No. 12) belong to the group of top processes controlling the abundances of primordial D,  $^3\text{He}$ ,  $^4\text{He}$ , and  $^7\text{Li}$  in SBBN. Below we show how the cross sections  $\sigma_B$  of these reactions in the presence of the magnetic field  $B$  are related to their unpolarized cross sections  $\sigma$ .

### A. $t(d,n)\alpha$ and $^3\text{He}(d,p)\alpha$ reactions

At energies relevant to BBN the  $t(d,n)\alpha$  reaction mainly proceeds in the  $S$ -wave channel, so the total angular momentum  $J$  of the reacting deuteron ( $I_d = 1$ ) and triton ( $I_t = 1/2$ ) can be  $3/2, 1/2$ . Accordingly, the reaction cross section in the presence of the magnetic field  $B$  is given by

$$\sigma_B = \sum_J \sum_{m_d, m_t, M} \xi_d(m_d) \xi_t(m_t) \left\langle 1m_d \frac{1}{2} m_t \middle| JM \right\rangle^2 \sigma_J. \quad (4)$$

In this equation,  $\langle 1m_d 1/2 m_t | JM \rangle^2$  is the squared Clebsch-Gordan coefficient determining the probability for the reacting nuclei to form the coupled state with momentum  $J$ , and  $\sigma_J$  is the partial cross section for this reaction proceeding through the  $J$  channel. Equation (4) can be reduced to the form [54]

$$\sigma_B = w_{3/2}(B) \sigma_{3/2} + w_{1/2}(B) \sigma_{1/2}, \quad (5)$$

where the functions  $w_{3/2}$  and  $w_{1/2}$  (the  $B$ -dependent weights of partial cross sections) are

$$w_{3/2} = a + 2b/3 + c/3, \quad w_{1/2} = b/3 + 2c/3, \quad (6)$$

and  $a = \xi_d(1)\xi_t(1/2) + \xi_d(-1)\xi_t(-1/2)$ ,  $b = \xi_d(0)$ ,  $c = \xi_d(1)\xi_t(-1/2) + \xi_d(-1)\xi_t(1/2)$ . For unpolarized deuterons and tritons  $a = b = c = 1/3$ , so the unpolarized  $t(d,n)\alpha$  cross section normally employed in astrophysical calculations is  $\sigma = 2\sigma_{3/2}/3 + \sigma_{1/2}/3$ . Therefore, Eq. (5) can be rewritten as

$$\sigma_B = \frac{3}{2} w_{3/2}(B) \sigma + \left[ w_{1/2}(B) - \frac{1}{2} w_{3/2}(B) \right] \sigma_{1/2}. \quad (7)$$

It is well known that at low energies the  $t(d,n)\alpha$  reaction predominantly proceeds through the ‘‘thermonuclear’’ ( $J^\pi, T$ ) = ( $3/2^+, 1/2$ ) state of the compound nucleus  $^5\text{He}$  at the excitation energy  $E^*$  of 16.84 MeV [55]. It was experimentally obtained (e.g., [56]) that  $\sim 99\%$  of the

total cross section is accounted for by the contribution of the  $3/2^+$  channel. At low energies thus  $\sigma_{1/2}/\sigma_{3/2} \ll 1$  and the role of the second term on the right-hand side of Eq. (7) can be neglected. It is worth noting here that Kulsrud *et al.* [57] first proposed to use deuteron and triton polarization for an enhancement of fusion rates in the laboratory DT plasma.

The above consideration is also applicable for the  $^3\text{He}(d,p)\alpha$  reaction. At low energies this reaction exhibits a resonant behavior and proceeds through the ( $3/2^+, 1/2$ ) state of the compound nucleus  $^5\text{Li}$  at the excitation energy  $E^*$  of 16.87 MeV [55]. So the reaction cross section can be described by Eq. (7) with  $w_{3/2}$  and  $w_{1/2}$  calculated for the  $d + ^3\text{He}$  nuclear system. A detailed study of the polarized  $^3\text{He}(d,p)\alpha$  reaction can be found in [58].

### B. $^3\text{He}(n,p)t$ and $^7\text{Be}(n,p)^7\text{Li}$ reactions

It was shown [59] that the cross sections of these ( $n,p$ ) reactions are well described by a superposition of resonant components with a comparatively small contribution of nonresonant terms.

For the  $^3\text{He}(n,p)t$  reaction, resonances corresponding to excited states of  $^4\text{He}$  with  $J^\pi = 0^+$  (at  $E^* = 20.21$  MeV),  $0^-$  (at  $E^* = 21.01$  MeV), and  $2^-$  (at  $E^* = 21.84$  and 23.33 MeV) [60] contribute to the cross section. These resonances supplemented with a  $1^+$  background component properly determine the reaction cross section at energies  $E \approx 0-7$  MeV [59]. The relative orbital momentum  $L$  and the total spin  $I$  of the reacting neutron ( $I_n = 1/2$ ) and  $^3\text{He}$  nucleus ( $I_{^3\text{He}} = 1/2$ ) are ( $L, I$ ) = ( $0, 0$ ) for  $J^\pi = 0^+$ , ( $1, 1$ ) for  $J^\pi = 0^-$ , ( $1, 1$ ) for  $J^\pi = 2^-$ , and ( $0, 1$ ) for  $J^\pi = 1^+$ . Having this in mind, the  $J^\pi$  partial cross section  $\sigma_{B, J^\pi}$  in the presence of the magnetic field  $B$  can be written in the following form:

$$\begin{aligned} \sigma_{B, J^\pi} &= \sum_{m_n, m_{^3\text{He}}, m_t, m_L, M} \xi_n(m_n) \xi_{^3\text{He}}(m_{^3\text{He}}) \\ &\times \left\langle \frac{1}{2} m_n \frac{1}{2} m_{^3\text{He}} \middle| Im_L \right\rangle^2 \langle Im_L m_L | JM \rangle^2 \sigma_{J^\pi} \\ &= w_J(B) \sigma_{J^\pi}. \end{aligned} \quad (8)$$

For the function  $w_J$  we obtain

$$\begin{aligned} w_J(B) &= c_{J,1} [\xi_n(-1/2) \xi_{^3\text{He}}(-1/2) + \xi_n(1/2) \xi_{^3\text{He}}(1/2)] \\ &+ c_{J,2} [\xi_n(-1/2) \xi_{^3\text{He}}(1/2) + \xi_n(1/2) \xi_{^3\text{He}}(-1/2)], \end{aligned} \quad (9)$$

where the coefficients  $\{c_{J,1}, c_{J,2}\}$  are  $\{0, 1/4\}$  for  $J^\pi = 0^+$ ,  $\{1/3, 1/6\}$  for  $J^\pi = 0^-$ ,  $\{5/3, 5/6\}$  for  $J^\pi = 2^-$ , and  $\{1, 1/2\}$  for  $J^\pi = 1^+$ . The total reaction cross section is

$$\sigma_B = \sum_{J^\pi} \sigma_{B, J^\pi}. \quad (10)$$

For unpolarized neutrons and  $^3\text{He}$  nuclei,  $\xi_n = \xi_{^3\text{He}} = 1/2$  and accordingly the unpolarized  $^3\text{He}(n, p)t$  cross section takes the form

$$\sigma = \frac{1}{8}\sigma_{0^+} + \frac{1}{4}\sigma_{0^-} + \frac{5}{4}\sigma_{2^-} + \frac{3}{4}\sigma_{1^+} \equiv \frac{1}{8}\sigma_{0^+} + \sigma_{021}. \quad (11)$$

It follows from Eq. (9) that for  $J^\pi = 0^-, 2^-, 1^+$

$$4w_0(B) = \frac{4}{5}w_2(B) = \frac{4}{3}w_1(B) \equiv w_{021}(B). \quad (12)$$

Taking this into account, one can obtain

$$\frac{\sigma_B}{\sigma} = \frac{\sigma_{B,0^+} + w_{021}(B)\sigma_{021}}{\sigma_{0^+}/8 + \sigma_{021}}. \quad (13)$$

Equation (13) demonstrates that  $\sigma_B = 8w_0\sigma$  for energies at which the  $J^\pi = 0^+$  channel is dominant ( $E \lesssim 0.1$  MeV) and  $\sigma_B = w_{021}(B)\sigma$  for energies at which the  $J^\pi = 0^+$  channel is subdominant ( $E \gtrsim 0.5$  MeV).

Similarly, one can describe the  $^7\text{Be}(n, p)^7\text{Li}$  reaction [59]. The  $J^\pi = 2^-$  excited state of the  $^8\text{Be}$  nucleus ( $E^* = 18.91$  MeV) located 10 keV above the  $n + ^7\text{Be}$  threshold [61] determines the cross section in the 0–0.2 keV energy range. Here, the reaction occurs in the  $S$ -wave channel; the total spin  $I$  of the reacting neutron and  $^7\text{Be}$  nucleus ( $I_{^7\text{Be}} = 3/2$ ) is 2. Including into consideration two overlapping  $3^+$  states of  $^8\text{Be}$  at excitation energies  $E^*$  of 19.07 MeV and 19.24 MeV (replaced by a single resonance) and also the  $3^+$  state at  $E^* = 21.5$  MeV leads to a good description of the  $^7\text{Be}(n, p)^7\text{Li}$  cross section at energies up to  $\sim 6$  MeV. In this wide energy region the reaction proceeds in the  $P$ -wave channel; the spin  $I$  of the  $n$ - $^7\text{Be}$  pair is 2. Having this in mind and neglecting a weak nonresonant contribution [59], the partial cross sections in the presence of the magnetic field  $B$  can be presented as the  $J^\pi = 2^-$  channel:

$$\begin{aligned} \sigma_{B,2^-} &= \sum_{m_n, m_{^7\text{Be}}, M} \xi_n(m_n)\xi_{^7\text{Be}}(m_{^7\text{Be}}) \\ &\quad \times \left\langle \frac{1}{2}m_n \frac{3}{2}m_{^7\text{Be}} | 2M \right\rangle^2 \sigma_{2^-} \\ &= w_2(B)\sigma_{2^-}, \end{aligned} \quad (14)$$

the  $J^\pi = 3^+$  channels:

$$\begin{aligned} \sigma_{B,3^+} &= \sum_{m_n, m_{^7\text{Be}}, m_I, m_L, M} \xi_n(m_n)\xi_{^7\text{Be}}(m_{^7\text{Be}}) \\ &\quad \times \left\langle \frac{1}{2}m_n \frac{3}{2}m_{^7\text{Be}} | 2m_I \right\rangle^2 \langle 2m_I 1m_L | 3M \rangle^2 \sigma_{3^+} \\ &= w_3(B)\sigma_{3^+}. \end{aligned} \quad (15)$$

The functions  $w_J$  ( $J = 2, 3$ ) are found to be

$$\begin{aligned} w_J(B) &= c_{J,1}[\xi_n(-1/2)\xi_{^7\text{Be}}(-3/2) + \xi_n(1/2)\xi_{^7\text{Be}}(3/2)] \\ &\quad + c_{J,2}[\xi_n(-1/2)\xi_{^7\text{Be}}(-1/2) + \xi_n(1/2)\xi_{^7\text{Be}}(1/2)] \\ &\quad + c_{J,3}[\xi_n(-1/2)\xi_{^7\text{Be}}(1/2) + \xi_n(1/2)\xi_{^7\text{Be}}(-1/2)] \\ &\quad + c_{J,4}[\xi_n(-1/2)\xi_{^7\text{Be}}(3/2) + \xi_n(1/2)\xi_{^7\text{Be}}(-3/2)], \end{aligned} \quad (16)$$

where the coefficients  $\{c_{J,1}, c_{J,2}, c_{J,3}, c_{J,4}\}$  are  $\{1, 3/4, 1/2, 1/4\}$  for  $J = 2$  and  $\{7/5, 21/20, 7/10, 7/20\}$  for  $J = 3$ . The total reaction cross section is

$$\sigma_B = \sigma_{B,2^-} + \sum \sigma_{B,3^+}. \quad (17)$$

If neutrons and  $^7\text{Be}$  nuclei are unpolarized,  $\xi_n = 1/2$ ,  $\xi_{^7\text{Be}} = 1/4$  and the unpolarized cross section has the form

$$\sigma = \frac{5}{8}\sigma_{2^-} + \frac{7}{8}\sum \sigma_{3^+}. \quad (18)$$

It follows from Eq. (16) that

$$\frac{8}{5}w_2(B) = \frac{8}{7}w_3(B) \equiv w_{23}(B) \quad (19)$$

and therefore Eqs. (17) and (18) give

$$\sigma_B = w_{23}(B)\sigma. \quad (20)$$

### C. $^7\text{Li}(p, \alpha)\alpha$ and $^7\text{Be}(n, \alpha)\alpha$ reactions

The law of parity conservation and symmetry properties of the  $\alpha$ - $\alpha$  system impose constraints on quantum numbers ( $L, I, J^\pi$ ) for the  $^7\text{Li}(p, \alpha)\alpha$  reaction. In particular,  $S$  partial waves in the system of colliding  $p$  and  $^7\text{Li}$  are forbidden and at energies relevant to BBN the reaction occurs in the  $P$ -wave channel. Considering that the total spin  $I$  of the proton ( $I_p = 1/2$ ) and  $^7\text{Li}$  ( $I_{^7\text{Li}} = 3/2$ ) can be 1 and 2, we easily obtain that for the  $^7\text{Li}(p, \alpha)\alpha$  process  $J^\pi = 0^+, 2^+$ . Accordingly, the partial cross section  $\sigma_{B, J^\pi}$  in the presence of the magnetic field  $B$  has the form

$$\begin{aligned} \sigma_{B, J^\pi} &= \sum_I \sum_{m_p, m_{^7\text{Li}}, m_I, m_L, M} \xi_p(m_p)\xi_{^7\text{Li}}(m_{^7\text{Li}}) \\ &\quad \times \left\langle \frac{1}{2}m_p \frac{3}{2}m_{^7\text{Li}} | Im_I \right\rangle^2 \langle Im_I 1m_L | JM \rangle^2 \sigma_{J^\pi} \\ &= w_J(B)\sigma_{J^\pi}. \end{aligned} \quad (21)$$

For the functions  $w_J$  ( $J = 0, 2$ ) we get



$$\begin{aligned}
 w_J = & c_{J,1}[\xi_p(-1/2)\xi_{7\text{Li}}(-3/2) + \xi_p(1/2)\xi_{7\text{Li}}(3/2)] \\
 & + c_{J,2}[\xi_p(-1/2)\xi_{7\text{Li}}(-1/2) + \xi_p(1/2)\xi_{7\text{Li}}(1/2)] \\
 & + c_{J,3}[\xi_p(-1/2)\xi_{7\text{Li}}(1/2) + \xi_p(1/2)\xi_{7\text{Li}}(-1/2)] \\
 & + c_{J,4}[\xi_p(-1/2)\xi_{7\text{Li}}(3/2) + \xi_p(1/2)\xi_{7\text{Li}}(-3/2)],
 \end{aligned} \quad (22)$$

where  $\{c_{J,1}, c_{J,2}, c_{J,3}, c_{J,4}\}$  are  $\{0, 1/12, 1/6, 1/4\}$  for  $J = 0$  and  $\{1, 7/6, 4/3, 3/2\}$  for  $J = 2$ . The total reaction cross section is

$$\sigma_B = \sigma_{B,0^+} + \sigma_{B,2^+} \quad (23)$$

while the cross section for unpolarized particles ( $\xi_p = 1/2$  and  $\xi_{7\text{Li}} = 1/4$ ) is given by

$$\sigma = \frac{1}{8}\sigma_{0^+} + \frac{5}{4}\sigma_{2^+}. \quad (24)$$

One can show that the above consideration is also valid for the  ${}^7\text{Be}(n, \alpha)\alpha$  reaction. Its cross section  $\sigma_{B,J^*}$  can be described by Eqs. (21) and (22) with the replacement of subscripts  $p$  and  ${}^7\text{Li}$  by  $n$  and  ${}^7\text{Be}$ , respectively.

### D. $p(n, \gamma)d$ reaction

Theoretical and experimental studies show that at energies relevant to BBN magnetic as well as electric transitions can contribute to the  $p(n, \gamma)d$  reaction mechanism (see, e.g., papers [52,62–65] and references therein). At neutron energies  $E_n < 0.1$  MeV the  $p(n, \gamma)d$  cross section is dominated by the  $np$  capture in the  ${}^1S_0$  state followed by the  $M1$  transition to the deuteron ground state  ${}^3S_1$ . In turn, at neutron energies  $E_n$  in excess of  $\sim 1$  MeV the reaction proceeds via the  $P$ -wave capture followed by the  $E1$  transition to the  ${}^3S_1$  channel. Three initial  $P$ -wave states  ${}^3P_0$ ,  ${}^3P_1$ , and  ${}^3P_2$  with partial amplitudes evaluated in [65] are involved in the  $P$ -wave capture. Finally, in the “intermediate” 0.1–1 MeV energy range both  $M1$  and  $E1$  mechanisms play roles, and their contributions to the total cross section were found to be comparable at  $E_n = 0.45$ –0.5 MeV. The respective partial cross sections  $\sigma_{M1}$  and  $\sigma_{E1}$  were precisely calculated in [65]. In the presence of the magnetic field  $B$  the  $p(n, \gamma)d$  cross section has the form

$$\sigma_B = w_M(B)\sigma_{M1} + w_E(B)\sigma_{E1}. \quad (25)$$

For the functions  $w_M$  and  $w_E$  we have obtained

$$\begin{aligned}
 w_M = & 2[\xi_p(-1/2)\xi_n(1/2) + \xi_p(1/2)\xi_n(-1/2)], \quad (26) \\
 w_E = & \frac{2}{3}[\xi_p(-1/2)\xi_n(1/2) + \xi_p(1/2)\xi_n(-1/2)] \\
 & + \frac{4}{3}[\xi_p(-1/2)\xi_n(-1/2) + \xi_p(1/2)\xi_n(1/2)]. \quad (27)
 \end{aligned}$$

In the case of unpolarized protons and neutrons,  $w_M = w_E = 1$  and Eq. (25) takes the form of the unpolarized cross section  $\sigma = \sigma_{M1} + \sigma_{E1}$ .

In the present paper we do not discuss the  $d(p, \gamma){}^3\text{He}$  radiative capture reaction. For an evaluation of its polarized cross section, we refer the reader to [52].

### E. $d(d, p)t$ and $d(d, n){}^3\text{He}$ reactions

Let  $\sigma_{m,n}$  be a partial cross section of the  $d + d$  reaction between deuterons with spin projections  $m$  and  $n$ . The only independent combinations of  $(m, n)$  are  $(1,1)$ ,  $(1,0)$ ,  $(1,-1)$ , and  $(0,0)$ . Therefore, in the presence of the magnetic field  $B$  the total cross section can be expressed as

$$\begin{aligned}
 \sigma_B = & w_{1,1}(B)\sigma_{1,1} + w_{1,0}(B)\sigma_{1,0} + w_{1,-1}(B)\sigma_{1,-1} \\
 & + w_{0,0}(B)\sigma_{0,0},
 \end{aligned} \quad (28)$$

where the partial weights  $w_{i,j}$  are

$$\begin{aligned}
 w_{1,1} = & \xi_d^2(-1) + \xi_d^2(1), \\
 w_{1,0} = & 2[\xi_d(-1)\xi_d(0) + \xi_d(1)\xi_d(0)], \\
 w_{1,-1} = & 2\xi_d(-1)\xi_d(1), \quad w_{0,0} = \xi_d^2(0).
 \end{aligned} \quad (29)$$

For unpolarized deuterons,  $w_{1,1} = w_{1,-1} = 2/9$ ,  $w_{1,0} = 4/9$ ,  $w_{0,0} = 1/9$ , and Eq. (28) gives the unpolarized cross section  $\sigma$  written in the standard form [66–68]

$$\sigma = \frac{1}{9}(2\sigma_{1,1} + 4\sigma_{1,0} + 2\sigma_{1,-1} + \sigma_{0,0}). \quad (30)$$

The quantity of particular interest is  $\sigma_{1,1}/\sigma$  [the so-called quintet suppression factor (QSF)] as it mainly determines how the cross section can change by a strong magnetic field. At the same time, the question of what QSF value is most realistic still remains a subject of discussions. In the absence of double polarized  $d + d$  fusion experiments [69], the theoretical analysis of the QSF is particularly important. Various calculations of  $\sigma_{1,1}/\sigma$  in different models, ranging from standard distorted-wave Born approximation methods to microscopic few-body approaches, have been performed to date. The QSF values available in the literature are summarized in [68]. In our study we employ recent results gotten from four-body Faddeev-Yakubovsky calculations [70]. The authors obtained a substantial decrease of  $\sigma_{1,1}/\sigma$  at energies relevant to BBN. In particular, for the  $d(d, n){}^3\text{He}$  reaction at the deuteron energy  $E_d = 100$  keV the value of  $\sigma_{1,1}/\sigma$  was found to be  $\sim 0.5$ .

## III. NUMERICAL RESULTS AND DISCUSSIONS

First, we specify the main points of the approach used by us to explore the PMF-induced polarization effects in BBN.

A model of randomly oriented and distributed thin-wall magnetic domains (or bubbles) [42,71] is chosen to

describe the PMF topology in the early Universe. According to it, the size of each domain is small compared with the event horizon, but is large enough so that one can consider the magnetic field to be uniform in the domain. It is assumed that the PMF effects on particle motion are similar in all domains. The magnetic field adiabatically decays due to expansion of the primordial plasma and the PMF strength  $B \propto R^{-2}$ , where  $R$  is the scale factor [48]. In the BBN epoch, the plasma temperature  $T \propto R^{-1}$  [2] that gives

$$B \simeq B_0 T_9^2, \quad (31)$$

where  $B_0$  is the field strength at the temperature  $T_9 (= T/10^9 \text{ K}) = 1$ .

Another point to be noted here is possible depolarization of reacting nuclei in the primordial plasma. It is known that standard mechanisms of particle depolarization in a plasma are binary collisions governed by spin-orbit or spin-spin interactions; magnetic field fluctuations and inhomogeneities [57]. The role of binary collisions was shown [72] to be normally unimportant. Furthermore, one can expect that the magnetic mechanisms of depolarization are also not significant for the field topology adopted by us. Although boundary distortions of the uniform field may occur at the magnetic bubble wall, their role can be neglected because the wall is assumed to be thin [42]. So the depolarization processes in the primordial plasma are likely to be weak and can reasonably be neglected.

Several constraints on the PMF strength  $B$  at the time of primordial nucleosynthesis are available in the literature. The cosmic microwave background limit gives  $B \sim 10^9 \text{ G}$  [48] while several detailed BBN-based considerations taking into account various PMF effects [42–45,49] lead to  $B$  in the range of  $3 \times 10^{10} - 2 \times 10^{11} \text{ G}$ . A specific value of  $B$  depends on what kinds of these effects are incorporated in the analysis. In particular, a recent constraint on  $B$  ( $2 \times 10^{11} \text{ G}$  at  $T_9 = 1$ ) [49] was obtained from rigorous

BBN simulations accurately allowing for the PMF effects through the field energy density, thermodynamic variables of electrons and positrons, and their time evolution.

It has been recognized [44–46] that the boost of cosmic expansion due to the contribution of the field energy density is the most important effect of the PMF. Following this conclusion, we have restricted our consideration to this effect by adding the magnetic energy density  $\rho_B = B^2/8\pi$  to the total energy density  $\rho = \rho_\gamma + (\rho_{e^-} + \rho_{e^+}) + \rho_\nu + \rho_b$  determining the Hubble expansion rate. To clarify the role of induced spin polarization, we have properly incorporated the spin-polarized cross sections  $\sigma_B$  obtained in Sec. II in a computational procedure based on the Kawano code [30]. This code has been modified so as to allow for nonthermal nuclear effects triggered by fast particles predominantly produced in the  $t(d,n)\alpha$ ,  $d(d,n)^3\text{He}$ ,  $d(d,p)t$ , and  $^3\text{He}(d,p)\alpha$  reactions [37,38]. In our calculations, we employed revised estimates [16,65] of the cross sections for key reactions listed in Table I, the neutron lifetime  $\tau_n = 880.3 \text{ s}$  and Newton's gravitational constant  $G_N = 6.673 \times 10^{-8} \text{ cm}^3 \text{ g}^{-1} \text{ s}^{-2}$  recommended by the Particle Data Group (2014) [73]. For the reduced particle magnetic moments  $g = \mu/\mu_N$  ( $\mu_N$  is the nuclear magneton) the following values were adopted:  $-1.913$  (for neutron),  $2.793$  (for proton),  $0.857$  (for deuteron),  $2.979$  (for triton),  $-2.127$  (for  $^3\text{He}$ ),  $3.256$  (for  $^7\text{Li}$ ), and  $-1.398$  (for  $^7\text{Be}$ ). Finally, the calculations were carried out with the baryon-to-photon ratio  $\eta_{\text{WMAP7}} = (6.16 \pm 0.15) \times 10^{-10}$  [5].

The results are presented in Table II. Shown are the primordial abundances of light elements obtained for several values of the PMF strength parameter  $B_0$ , Eq. (31), in the range of  $10^9$ – $10^{12} \text{ G}$ . The SBBN scenario without magnetic field is given by the column for  $B_0 = 0$ . Subscripts and superscripts at each abundance indicate its change when the baryon-to-photon ratio  $\eta_{\text{WMAP7}}$  spans the  $(6.16 - 0.15) \times 10^{-10} - (6.16 + 0.15) \times 10^{-10}$  error range. Table II shows that the abundances  $A/H$  exhibit different sensitivities to the magnetic field and deviate from

TABLE II. The primordial abundances of light elements at different values of the PMF strength parameter  $B_0 = B/T_9^2$ . The field effects are taken into account through the magnetic energy density  $\rho_B$  and the spin-polarized cross sections  $\sigma_B$  of key nuclear reactions. Subscripts and superscripts at each abundance indicate its change when  $\eta_{\text{WMAP7}}$  spans the  $(6.16 - 0.15) \times 10^{-10} - (6.16 + 0.15) \times 10^{-10}$  error range.

| Element                                      | $B_0$ (G)                 |                           |                           |                           |                           | Observations<br>Ref. [73] |
|--|---------------------------|---------------------------|---------------------------|---------------------------|---------------------------|---------------------------|
|  | 0                         | $10^9$                    | $10^{10}$                 | $10^{11}$                 | $10^{12}$                 |                           |
| D/H ( $\times 10^{-5}$ )                     | $2.522_{-0.096}^{+0.102}$ | $2.522_{-0.096}^{+0.102}$ | $2.523_{-0.096}^{+0.101}$ | $2.589_{-0.098}^{+0.104}$ | $8.747_{-0.338}^{+0.361}$ | $2.53 \pm 0.04$           |
| T/H ( $\times 10^{-8}$ )                     | $7.651_{-0.300}^{+0.319}$ | $7.651_{-0.300}^{+0.319}$ | $7.653_{-0.300}^{+0.319}$ | $7.869_{-0.309}^{+0.325}$ | $29.21_{-1.160}^{+1.240}$ |                           |
| $^3\text{He}/\text{H}$ ( $\times 10^{-5}$ )  | $1.003_{-0.014}^{+0.015}$ | $1.003_{-0.014}^{+0.015}$ | $1.003_{-0.013}^{+0.015}$ | $1.013_{-0.015}^{+0.014}$ | $1.628_{-0.027}^{+0.028}$ | $1.1 \pm 0.2^a$           |
| $Y_p$ ( $\times 10^{-1}$ )                   | $2.446_{-0.002}^{+0.002}$ | $2.446_{-0.002}^{+0.002}$ | $2.446_{-0.002}^{+0.003}$ | $2.459_{-0.002}^{+0.003}$ | $3.198_{-0.002}^{+0.002}$ | $2.465 \pm 0.097$         |
| $^6\text{Li}/\text{H}$ ( $\times 10^{-14}$ ) | $1.090_{-0.038}^{+0.041}$ | $1.090_{-0.038}^{+0.041}$ | $1.091_{-0.039}^{+0.041}$ | $1.126_{-0.040}^{+0.042}$ | $5.239_{-0.193}^{+0.205}$ |                           |
| $^7\text{Li}/\text{H}$ ( $\times 10^{-10}$ ) | $4.519_{-0.228}^{+0.231}$ | $4.519_{-0.228}^{+0.231}$ | $4.518_{-0.228}^{+0.231}$ | $4.406_{-0.224}^{+0.227}$ | $1.625_{-0.017}^{+0.024}$ | $1.6 \pm 0.3$             |

<sup>a</sup>This value taken from [74] gives a constraint on primordial  $^3\text{He}$  deduced from observations in our Galaxy.

the SBBN predictions at  $B_0 \gtrsim 10^{10}$  G. Their dependencies on  $B_0$  are in agreement with those obtained (and explained) in a recent paper [49].

The partial effects on the abundances through the magnetic energy density  $\rho_B$  and through the spin-polarized cross sections  $\sigma_B$  have been clarified. Our analysis has revealed that the major part of abundance change  $\delta_{A/H}$  comes from  $\rho_B$  while the contribution of  $\sigma_B$  to  $\delta_{A/H}$  proves to be at most 0.01%. Furthermore, rough estimations indicate that the inclusion into consideration of the other PMF effects noted above would not significantly change the relative role of induced spin polarization in the element production, remaining on the same level of magnitude. Table II also shows that this value is smaller than the abundance uncertainties (of several percent) resulting from the error of  $\eta_{\text{WMAP7}}$  determination.

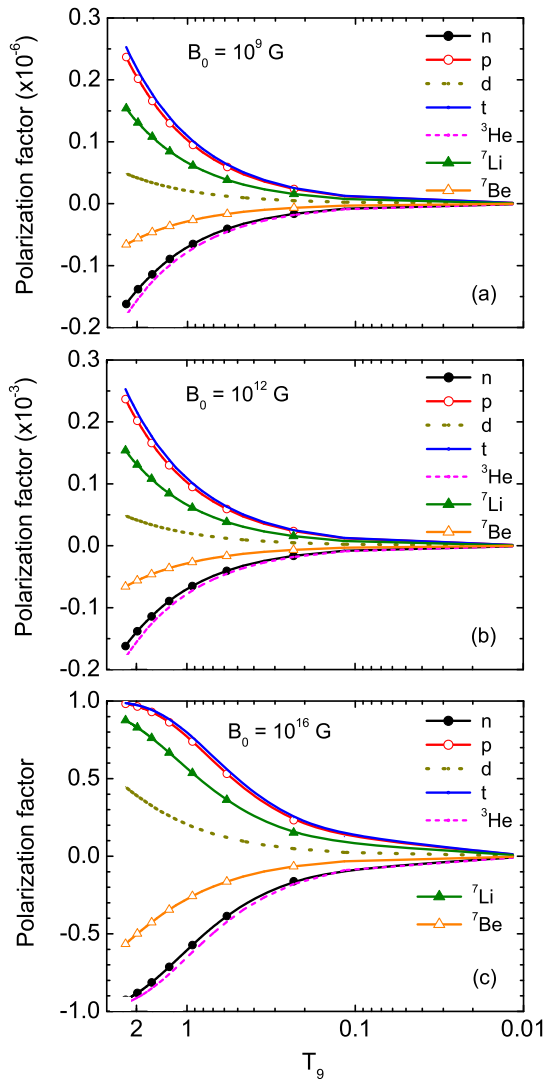


FIG. 1 (color online). The nuclear polarization factors  $P_{\text{nuc}}$  for nucleons and light nuclei at different values of the magnetic field strength parameter  $B_0$  as a function of the Universe temperature. (a)  $B_0 = 10^9$  G, (b)  $B_0 = 10^{12}$  G, (c)  $B_0 = 10^{16}$  G.

The obtained  $\sigma_B$  effect is consistent with data presented in Fig. 1. It shows the nuclear polarization factors  $P_{\text{nuc}}$ , Eq. (1), for particles involved in the key BBN reactions given in Table I. In this figure, three values of the strength parameter  $B_0 = 10^9$ ,  $10^{12}$ , and  $10^{16}$  G are considered. We note that the overall drop of  $|P_{\text{nuc}}|$  with decreasing temperature is accounted for by the magnetic field adiabatic decay as the Universe expands. It is seen that for  $B_0 \leq 10^{12}$  G being considered in Table II the values of  $|P_{\text{nuc}}|$  are at most  $\sim 0.02\%$ , so they are close to the abundance changes caused by the polarized cross sections  $\sigma_B$ . In the meantime, Fig. 1(c) demonstrates that a high degree of polarization—from several tens of percent and up to one hundred percent (depending on a type of particle)—can be reached in the magnetic field with  $B_0 = 10^{16}$  G. This suggests that overcritical magnetic fields with  $B_0 > B_C$ , where  $B_C = m_c^2/e = 4.41 \times 10^{13}$  G is the critical strength above which quantized cyclotron states appear [47], can essentially affect the reaction cross sections discussed in Sec. II.

The respective results for some of these processes are shown in Figs. 2–6. In particular, Fig. 2 presents the results obtained for the  $t(d, n)\alpha$  and  ${}^3\text{He}(d, p)\alpha$  reactions. Shown are the ratios of the reaction cross sections  $\sigma_B$  allowing for

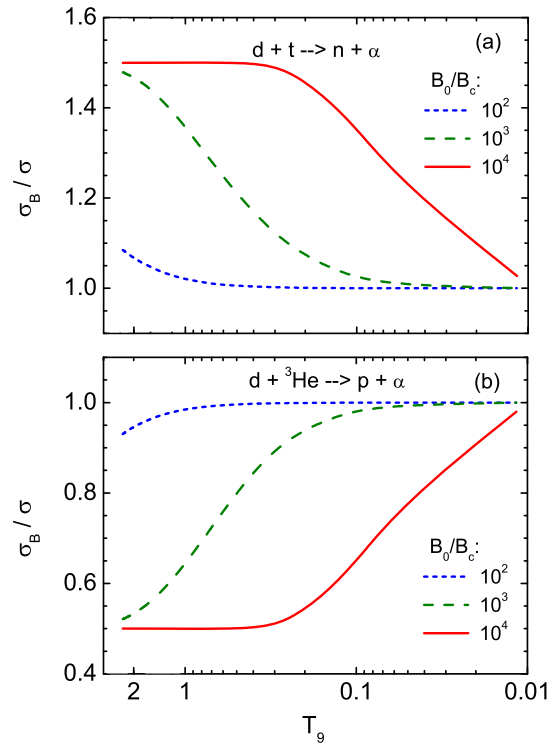


FIG. 2 (color online). The magnetic field effect on the  $t(d, n)\alpha$  and  ${}^3\text{He}(d, p)\alpha$  reactions as a function of the Universe temperature. Shown are the ratios of the cross sections  $\sigma_B$  allowing for induced particles polarization to the unpolarized cross sections  $\sigma$ . The field strength parameter  $B_0$  is expressed in units of  $B_C = 4.41 \times 10^{13}$  G. (a) The  $t(d, n)\alpha$  reaction. (b) The  ${}^3\text{He}(d, p)\alpha$  reaction.

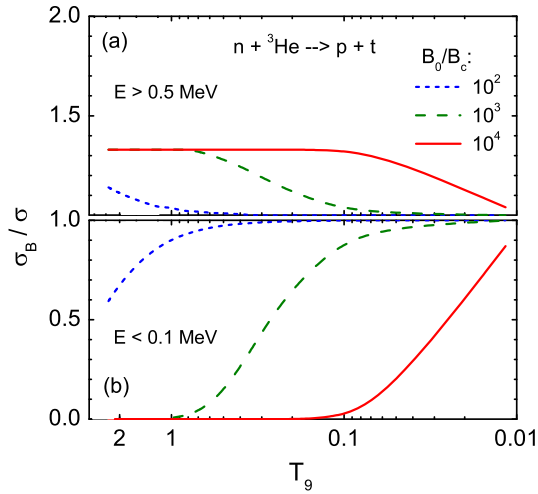


FIG. 3 (color online). The magnetic field effect on the  ${}^3\text{He}(n, p)t$  reaction (for additional explanations, see the caption to Fig. 2). In the energy regions being considered  $\sigma_B/\sigma$  can be assumed to be independent of  $E$ .

induced particle polarization to the unpolarized cross sections  $\sigma$ . It is seen that the overcritical magnetic field noticeably affects the cross sections and, in agreement with Fig. 1, the impact is most significant at high temperatures. Furthermore, the effects prove to be opposite for the two processes—the magnetic field enhances the  $t(d, n)\alpha$  reaction and suppresses the  ${}^3\text{He}(d, p)\alpha$  one. This suppression results from different signs of the  ${}^3\text{He}$  and  $d$  magnetic moments that favors opposite orientation of the particle spins, at which the resonant  ${}^3\text{He}(d, p)\alpha$  reaction cannot effectively proceed. It follows from Eq. (7) that for the completely polarized nuclei  $\sigma_B/\sigma \approx 3/2$  and  $1/2$  for the  $t(d, n)\alpha$  and  ${}^3\text{He}(d, p)\alpha$  reactions, respectively. Figure 2 demonstrates that such values of  $\sigma_B/\sigma$  are attained at  $B_0 \gtrsim 10^3 B_C$ . The results obtained for the  ${}^3\text{He}(n, p)t$  reaction are shown in Fig. 3. Although the ratio  $\sigma_B/\sigma$  for this reaction in general depends on  $B_0$ ,  $T_9$ , and energy

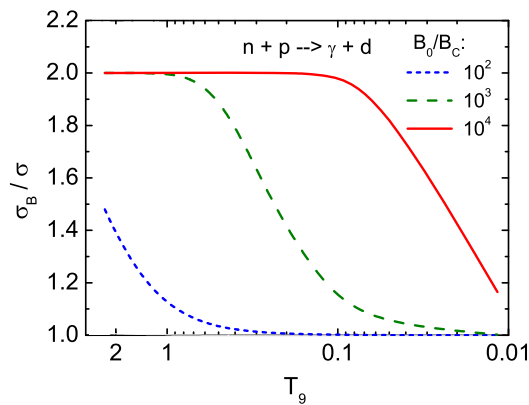


FIG. 4 (color online). The magnetic field effect on the  $p(n, \gamma)d$  cross section (the  $M1$  transition component). For additional explanations, see Eq. (25) and the caption to Fig. 2.

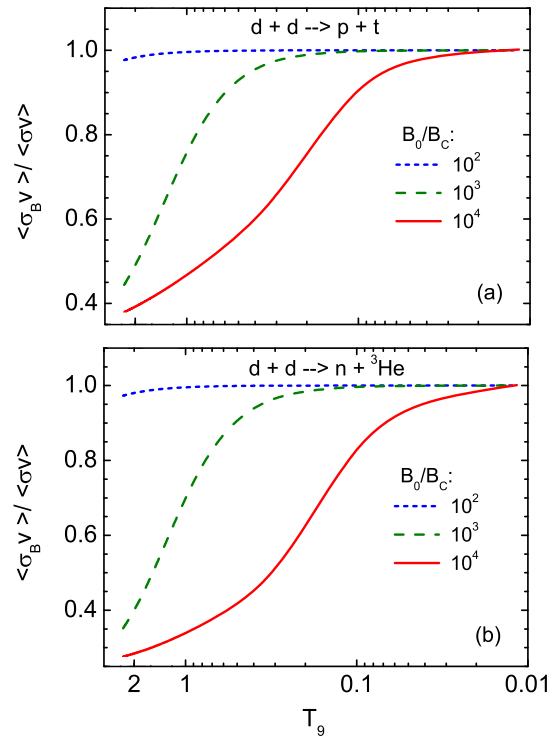


FIG. 5 (color online). The magnetic field effect on the  $d(d, p)t$  and  $d(d, n){}^3\text{He}$  reactions. Shown are the rate parameter ratios  $\langle\sigma_B v\rangle/\langle\sigma v\rangle$  as a function of the Universe temperature. (a) The  $d(d, p)t$  reaction. (b) The  $d(d, n){}^3\text{He}$  reaction.

$E$ , there are two energy regions—below 0.1 MeV and above 0.5 MeV—where  $\sigma_B/\sigma$  can be assumed to be energy independent (see Sec. II). These cases are considered in Fig. 3. It is seen that at energies  $E > 0.5$  MeV the  ${}^3\text{He}(n, p)t$  reaction is enhanced while at  $E < 0.1$  MeV it is suppressed. The latter is of particular interest as Fig. 3(b)

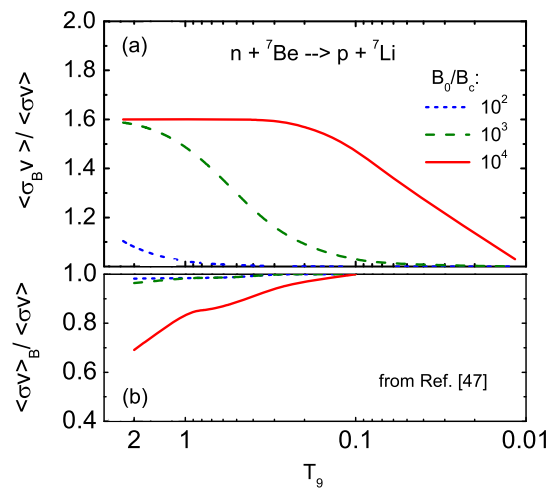


FIG. 6 (color online). The magnetic field effects on the  ${}^7\text{Be}(n, p){}^7\text{Li}$  reaction rate parameter caused by two different mechanisms (see explanations in the text). (a) Present paper. (b) Results [49].



shows that the field with  $B_0 \gtrsim 10^3 B_C$  can almost block this reaction responsible for the interconversion of  $A = 3$  nuclei. The magnetic field effect on the  $p(n, \gamma)d$  reaction determining the starting point of BBN is presented in Fig. 4. Here we show the results for the  $M1$  transition cross section component—the first term on the right-hand side of Eq. (25)—playing the dominant role in an important energy region  $E_n < 0.5$  MeV. An appreciable enhancement of the  $p(n, \gamma)d$  cross section by a factor of 1.5–2 is observed at high temperatures.

Figures 5 and 6(a) demonstrate the magnetic field effects on energy-averaged quantities—the reaction rate parameters  $\langle \sigma_B v \rangle$  calculated with Maxwellian particle distribution functions. Shown are the values of  $\langle \sigma_B v \rangle / \langle \sigma v \rangle$  for three processes. Figure 5 presents the results for the  $d(d, p)t$  and  $d(d, n)^3\text{He}$  reactions. A significant suppression of both processes clearly manifests at  $B_0 > 10^2 B_C$ . Figure 6(a) shows the results for the  ${}^7\text{Be}(n, p){}^7\text{Li}$  reaction. For this process, an enhancement of the rate parameter is observed. It follows from Eq. (20) that for the completely polarized neutron and  ${}^7\text{Be}$  nucleus  $\sigma_B/\sigma = 1.6$ . As seen from Fig. 6(a), this value is attained at  $B_0 \gtrsim 10^3 B_C$ . Kawasaki and Kusakabe [49] examined a different effect of overcritical magnetic fields on  $\langle \sigma v \rangle$  resulting from a discretization of momentum on the plane perpendicular to the field direction. The authors calculated the  ${}^7\text{Be}(n, p){}^7\text{Li}$  rate parameter with a quantized distribution function of  ${}^7\text{Be}$ , assuming that the field impact on the reaction cross section can be neglected, i.e.,  $\sigma_B = \sigma$ . For convenience, we denote this quantity as  $\langle \sigma v \rangle_B$ . The ratio  $\langle \sigma v \rangle_B / \langle \sigma v \rangle$  is presented in Fig. 6(b). A comparison of  $\langle \sigma_B v \rangle / \langle \sigma v \rangle$  in Fig. 6(a) with  $\langle \sigma v \rangle_B / \langle \sigma v \rangle$  in Fig. 6(b) shows that the effects caused by the two mechanisms being discussed are essentially different. First of all, for the given reaction they prove to be opposite. Besides, the magnetic field effect through the polarized cross section is more strong (and even fully dominant at  $B_0 \leq 10^3 B_C$ ) than that through the  ${}^7\text{Be}$  quantized distribution function. These conclusions however concern the particular  ${}^7\text{Be}(n, p){}^7\text{Li}$  reaction and cannot be qualified as a general rule. Each process needs a special consideration.

#### IV. CONCLUSIONS

We have examined the spin polarization of nucleons and light nuclei with  $A \leq 7$  induced by magnetic fields in the primordial plasma. The influence of this polarization on reaction cross sections of importance in BBN and primordial element abundances has been clarified. Summarizing the results obtained, we conclude the following.

For the subcritical magnetic field with the strength parameter  $B_0 < B_C = 4.41 \times 10^{13}$  G, the degree of particle polarization is insufficient to appreciably affect the cross sections of reactions controlling the production of light elements. As a consequence, the BBN simulations allowing for magnetic field effects through the field energy density and the spin-polarized cross sections have revealed that the latter mechanism plays a minor role, changing light element abundances at most by 0.01%.

For the overcritical magnetic field with  $B_0 > B_C$ , the induced particle polarization can reach several tens of percent and noticeably change (increase or decrease) the cross sections of key BBN reactions listed in Table I. These changes begin to manifest at  $B_0 \sim 10^{15}$  G. Two particular cases are worth noting here. It has been obtained that the magnetic field can increase the  $p(n, \gamma)d$  cross section (relevant to the starting point of BBN) by a factor of 2 and at the same time almost block the  ${}^3\text{He}(n, p)t$  reaction responsible for the interconversion of  $A = 3$  nuclei in the early Universe.

The overall picture of nucleosynthesis under these conditions is hardly possible to realize as overcritical magnetic fields are unlikely to fill the early Universe. The energy density of these fields would considerably increase the total energy contents that in turn would strongly boost the expansion rate. However, locally the magnetic field could be very large, so the spin polarization effects may become important in nonstandard BBN scenarios considering the existence of domains inside which the field can reach  $\sim 10^{15}$  G.

[1] D. N. Spergel *et al.*, *Astrophys. J. Suppl. Ser.* **148**, 175 (2003).  
 [2] R. V. Wagoner, W. A. Fowler, and F. Hoyle, *Astrophys. J.* **148**, 3 (1967).  
 [3] R. V. Wagoner, *Astrophys. J. Suppl. Ser.* **18**, 247 (1969).  
 [4] D. N. Spergel *et al.*, *Astrophys. J. Suppl. Ser.* **170**, 377 (2007).  
 [5] E. Komatsu *et al.*, *Astrophys. J. Suppl. Ser.* **192**, 18 (2011).  
 [6] G. Hinshaw *et al.*, *Astrophys. J. Suppl. Ser.* **208**, 19 (2013).

[7] It should be noted here that, although the lithium problem has not been resolved within SBBN, some nonstandard BBN scenarios propose pathways to alleviate the  ${}^7\text{Li}$  discrepancy (see, e.g., reviews [8–11] and references therein).  
 [8] B. D. Fields, *Annu. Rev. Nucl. Part. Sci.* **61**, 47 (2011).  
 [9] M. Pospelov and J. Pradler, *Annu. Rev. Nucl. Part. Sci.* **60**, 539 (2010).  
 [10] F. Iocco, G. Mangano, G. Miele, O. Pisanti, and P. D. Serpico, *Phys. Rep.* **472**, 1 (2009).

- [11] G. Steigman, *Annu. Rev. Nucl. Part. Sci.* **57**, 463 (2007).
- [12] A. Coc, J.-P. Uzan, and E. Vangioni, *J. Cosmol. Astropart. Phys.* **10** (2014) 050.
- [13] P. A. R. Ade *et al.* (Planck Collaboration), *Astron. Astrophys.* **571**, A16 (2014).
- [14] It is worthwhile to note that another analysis of BBN with Planck data [15] revealed a discrepancy between theoretical and observed abundances of  $^4\text{He}$ .
- [15] R. Ichimasa, R. Nakamura, M. Hashimoto, and K. Arai, *Phys. Rev. D* **90**, 023527 (2014).
- [16] R. H. Cyburt, *Phys. Rev. D* **70**, 023505 (2004).
- [17] P. D. Serpico, S. Esposito, F. Iocco, G. Mangano, G. Miele, and O. Pisanti, *J. Cosmol. Astropart. Phys.* **12** (2004) 010.
- [18] A. Coc, E. Vangioni-Flam, P. Descouvemont, A. Adahchour, and C. Angulo, *Astrophys. J.* **600**, 544 (2004).
- [19] R. H. Cyburt, B. D. Fields, and K. A. Olive, *J. Cosmol. Astropart. Phys.* **11** (2008) 012.
- [20] R. N. Boyd, C. R. Brune, G. M. Fuller, and C. J. Smith, *Phys. Rev. D* **82**, 105005 (2010).
- [21] A. Coc, S. Goriely, Yi Xu, M. Saimpert, and E. Vangioni, *Astrophys. J.* **744**, 158 (2012).
- [22] N. Chakraborty, B. D. Fields, and K. A. Olive, *Phys. Rev. D* **83**, 063006 (2011).
- [23] O. S. Kirsebom and B. Davids, *Phys. Rev. C* **84**, 058801 (2011).
- [24] R. H. Cyburt and M. Pospelov, *Int. J. Mod. Phys. E* **21**, 1250004 (2012).
- [25] C. Brogini, L. Canton, G. Fiorentini, and F. L. Villante, *J. Cosmol. Astropart. Phys.* **06** (2012) 030.
- [26] P. D. O'Malley *et al.*, *Phys. Rev. C* **84**, 042801(R) (2011).
- [27] F. Hammache *et al.*, *Phys. Rev. C* **88**, 062802(R) (2013).
- [28] A. Coc, P. Descouvemont, K. A. Olive, J.-P. Uzan, and E. Vangioni, *Phys. Rev. D* **86**, 043529 (2012).
- [29] J. C. Berengut, E. Epelbaum, V. V. Flambaum, C. Hanhart, U. G. Meißner, J. Nebreda, and J. R. Peláez, *Phys. Rev. D* **87**, 085018 (2013).
- [30] L. Kawano, Report No. FERMILAB-PUB-92/04-A, 1992 (unpublished).
- [31] F. Iocco, G. Mangano, G. Miele, O. Pisanti, and P. D. Serpico, *Phys. Rev. D* **75**, 087304 (2007).
- [32] H. S. Picker, *Phys. Rev. C* **30**, 1751 (1984).
- [33] V. T. Voronchev, Research notice (2013) (unpublished).
- [34] B. Wang, C. A. Bertulani, and A. B. Balantekin, *Phys. Rev. C* **83**, 018801 (2011).
- [35] C. A. Bertulani, J. Fuqua, and M. S. Hussein, *Astrophys. J.* **767**, 67 (2013).
- [36] V. T. Voronchev, Y. Nakao, and M. Nakamura, *Astrophys. J.* **725**, 242 (2010).
- [37] Y. Nakao, K. Tsukida, and V. T. Voronchev, *Phys. Rev. D* **84**, 063016 (2011).
- [38] V. T. Voronchev, Y. Nakao, K. Tsukida, and M. Nakamura, *Phys. Rev. D* **85**, 067301 (2012).
- [39] R. F. O'Connell and J. J. Matese, *Nature (London)* **222**, 649 (1969).
- [40] G. Greenstein, *Nature (London)* **223**, 938 (1969).
- [41] J. J. Matese and R. F. O'Connell, *Astrophys. J.* **160**, 451 (1970).
- [42] B. Cheng, D. N. Schramm, and J. W. Truran, *Phys. Rev. D* **49**, 5006 (1994).
- [43] D. Grasso and H. R. Rubinstein, *Astropart. Phys.* **3**, 95 (1995).
- [44] B. Cheng, A. V. Olinto, D. N. Schramm, and J. W. Truran, *Phys. Rev. D* **54**, 4714 (1996).
- [45] D. Grasso and H. R. Rubinstein, *Phys. Lett. B* **379**, 73 (1996).
- [46] P. J. Kernan, G. D. Starkman, and T. Vachaspati, *Phys. Rev. D* **54**, 7207 (1996).
- [47] D. Grasso and H. R. Rubinstein, *Phys. Rep.* **348**, 163 (2001).
- [48] A. Kandus, K. E. Kunze, and C. G. Tsagas, *Phys. Rep.* **505**, 1 (2011).
- [49] M. Kawasaki and M. Kusakabe, *Phys. Rev. D* **86**, 063003 (2012).
- [50] D. G. Yamazaki and M. Kusakabe, *Phys. Rev. D* **86**, 123006 (2012).
- [51] D. G. Yamazaki, T. Kajino, G. J. Mathews, and K. Ichiki, *Phys. Rep.* **517**, 141 (2012).
- [52] E. Tomasi-Gustafsson and M. P. Rekaló, *Phys. Part. Nucl.* **33**, 436 (2002).
- [53] M. E. Rose, *Phys. Rev.* **75**, 213 (1949).
- [54] R. M. Kulsrud, E. J. Valeo, and S. C. Cowley, *Nucl. Fusion* **26**, 1443 (1986).
- [55] D. R. Tilley, C. M. Cheves, J. L. Godwin, G. M. Hale, H. M. Hofmann, J. H. Kelley, C. G. Sheu, and H. R. Weller, *Nucl. Phys.* **A708**, 3 (2002).
- [56] R. E. Brown, N. Jarmie, and N. Hardekopf, *IEEE Trans. Nucl. Sci.* **30**, 1164 (1983).
- [57] R. M. Kulsrud, H. P. Furth, E. J. Valeo, and M. Goldhaber, *Phys. Rev. Lett.* **49**, 1248 (1982).
- [58] M. P. Rekaló and E. Tomasi-Gustafsson, *Phys. Rev. C* **57**, 2870 (1998).
- [59] A. Adahchour and P. Descouvemont, *J. Phys. G* **29**, 395 (2003).
- [60] D. R. Tilley, H. R. Weller, and G. M. Hale, *Nucl. Phys.* **A541**, 1 (1992).
- [61] D. R. Tilley, J. H. Kelley, J. L. Godwin, D. J. Millener, J. E. Purcell, C. G. Sheu, and H. R. Weller, *Nucl. Phys.* **A745**, 155 (2004).
- [62] T. S. Suzuki, Y. Nagai, T. Shima, T. Kikuchi, H. Sato, T. Kii, and M. Igashira, *Astrophys. J. Lett.* **439**, L59 (1995).
- [63] Y. Nagai, T. S. Suzuki, T. Kikuchi, T. Shima, T. Kii, H. Sato, and M. Igashira, *Phys. Rev. C* **56**, 3173 (1997).
- [64] G. Rupak, *Nucl. Phys.* **A678**, 405 (2000).
- [65] S. Ando, R. H. Cyburt, S. W. Hong, and C. H. Hyun, *Phys. Rev. C* **74**, 025809 (2006).
- [66] G. M. Hale and G. D. Doolen, Los Alamos Report No. LA-9971-MS, 1984.
- [67] K. A. Fletcher, Z. Ayer, T. C. Black, R. K. Das, H. J. Karwowski, E. J. Ludwig, and G. M. Hale, *Phys. Rev. C* **49**, 2305 (1994).
- [68] H. Paetz gen. Schieck, *Few-Body Syst.* **54**, 2159 (2013).
- [69] K. Grigoryev *et al.*, *J. Phys. Conf. Ser.* **295**, 012168 (2011).
- [70] A. Deltuva and A. C. Fonseca, *Phys. Rev. C* **81**, 054002 (2010).
- [71] T. Tajima, S. Cable, K. Shibata, and R. M. Kulsrud, *Astrophys. J.* **390**, 309 (1992).
- [72] L. Wolfenstein, *Phys. Rev.* **75**, 1664 (1949).
- [73] K. A. Olive *et al.* (Particle Data Group), *Chin. Phys. C* **38**, 090001 (2014).
- [74] T. M. Bania, R. T. Rood, and D. S. Balse, *Nature (London)* **415**, 54 (2002).